Pergamon

Tetrahedron: *Asymmetry* 11 (2000) 337–362

TETRAHEDRON: *ASYMMETRY*

TETRAHEDRON: ASYMMETRY REPORT NUMBER 46

# Examining the secondary structures of unnatural peptides and carbohydrate-based compounds utilizing circular dichroism

Katherine D. McReynolds † and Jacquelyn Gervay-Hague *

*The University of Arizona, Department of Chemistry, Tucson, AZ 85721, USA*

Received 22 November 1999; accepted 3 December 1999

**Abstract**

This review focuses on the use of CD in elucidating structure in oligo- and polysaccharides, unnatural β- and γ-peptides, and both natural and unnatural oligo- and polymers composed of *N*-acetyl neuraminic acid. CD in conjunction with other techniques such as NMR and molecular modeling has been successfully used to gain a clearer picture of the hydrogen-bonding interactions, and conformational information of molecules that are not accessible by X-ray crystallography. The use of the peak-to-trough analysis within each class of oligomers has been an integral part of the analysis, and has provided interesting insights into the conformational changes that occur within oligomers with varied chain lengths. Continued studies in this relatively new area of research will add to the knowledge base that correlates circular dichroism data with other spectroscopic techniques ultimately facilitating secondary structure characterization. 

**Contents**



## 1. Introduction

The determination of secondary structure in macromolecules is an increasingly important area of research. Crystallography is arguably the most definitive method for determining structure; however, it is not always possible to obtain materials in an appropriate form for this technique. Furthermore,

* Corresponding author. E-mail: gervay@u.arizona.edu

† Present address: Department of Biological Chemistry, University of California School of Medicine, One Shields Avenue Davis, CA 95616, USA.

0957-4166/00/$ - see front matter 
*PII:* S0957-4166(99)00560-1

solution phase conformations of various compounds may differ from the conformations adopted in the crystal structure. Solution phase structure determination is greatly facilitated by NMR spectroscopy, and certainly for protein structure determination circular dichroism (CD) has played an important role.[1] CD has also been used to study oligo- and polysaccharides in solution. More recently, CD has been used to elucidate secondary structures in unnatural amide-linked compounds. This review focuses on the use of CD in elucidating structure in oligo- and polysaccharides, unnatural β- and γ-peptides, and both natural and unnatural oligo- and polymers composed of *N*-acetyl neuraminic acid.

Circular dichroism, or CD, is an empirical technique used to elucidate the secondary structures of oligomeric and polymeric materials. CD is a chiroptical method requiring the molecule under analysis to possess optical activity. The first practical use of a CD spectropolarimeter was reported in 1965, when Holzwarth and Doty recorded the CD spectrum of an α-helix.[2] Today, CD analysis is standard practice in structure determination of peptides, proteins, nucleic acids, and oligo- and polysaccharides. The common property that all of these biomolecules possess is chirality.

CD is defined as the difference in absorption between left- and right-circularly polarized light when an asymmetric molecule lies in the path of these light forms. In general, the velocity of both light waves is diminished by the interaction with a chiral molecule; however, one will be more retarded than the other, resulting in a net absorption band.[3] The difference in the absorption ($\Delta A\lambda$) is proportional to the concentration of the sample (c), the path length (l), and the difference in molar absorptivity ($\Delta\varepsilon$) according to Beer's law (Fig. 1).

$$A_L(\lambda) - A_R(\lambda) = \Delta A(\lambda) = \{\varepsilon_L(\lambda) - \varepsilon_R(\lambda)\}lc = \Delta\varepsilon(\lambda)lc$$

Fig. 1. Beer's law as applied to circular dichroism. The subscripts, R and L, represent the handedness of the light

The circular dichroic behavior of a molecule is measured as the ellipticity, θ. The term ellipticity refers to the elliptical shape of the electric vector traced when one form of the light is absorbed by the sample in a different manner than the other. The ellipticity (commonly given in the units of millidegrees, mdeg) of a molecule is transformed at each wavelength into a value that depends upon the molecular mass, M (in g/mol), the concentration, c (g/L), and the pathlength, l (mm). The resultant values, known as the molar ellipticity, [θ], are those commonly reported in the literature for the CD of biomolecules (Fig. 2).

$$[\theta] = (\theta M)/cl$$

Fig. 2. The equation utilized to transform raw ellipticity data, θ, into the molar ellipticity, [θ]

Several solvents may be employed in the collection of CD spectra. However, the transparency of the given solvent, within the wavelength range measured, can be important. Certain molecules may yield CD spectra with altered bands in different solvents, depending on the degree of interaction of the chiral molecule with the solvent molecules. In some cases, the solvent effects may be so drastic as to give rise to inverted spectral bands.[4] W. C. Johnson Jr. provides an excellent review about the scope and usefulness of solvents and other additives in CD.[5]

The previous discussion provides the background information necessary to understand the technique of circular dichroism in a general fashion. Many recent review articles and book chapters exist that give a more thorough handling of the basic principles of CD; some specifically with applications in the area of secondary structural analyses of peptides and proteins.[5–9] Carbohydrate CD has also been extensively covered, with regards to the determination of the structural characteristics of monosaccharides and polysaccharides.[3,10,11] The reader is referred to these publications for further information.

## 2. Circular dichroism in defining the secondary structure of carbohydrates

The CD of carbohydrates is an intriguing and challenging area of research. The mechanics of data analysis has proven to be more problematic for carbohydrates than that posed for peptides and proteins. This is due to inherent differences in the structure of carbohydrates and proteins. The CD of peptides and proteins relies on the absorbance of the amide-linked backbone of the molecule. Naturally occurring peptides and proteins are composed of α-amino acids, which give rise to a regular pattern of homologous repeating chromophores that differ only in the R groups appended at $C_\alpha$. Carbohydrates differ not only in the type and spacing of the chromophores but also in the connectivity. Both linear and branched carbohydrates can exist. Furthermore, both isomeric forms of carbohydrates occur in nature, namely the common D form and the less common L form, while proteins are comprised of only the L amino acids. In polysaccharides, the glycosidic linkage angles ϕ and ψ define the conformation of the molecule because the remaining structure has a set geometry determined by the sugar rings.[3] Fig. 3 depicts the ϕ, ψ dihedral angles about the glycosidic bond.

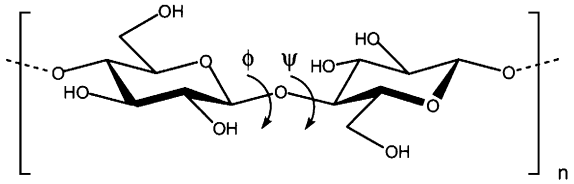


Fig. 3. Dihedral angles, ϕ and ψ, of the glycosidic bond in oligo- and polysaccharides. The ϕ dihedral angle is defined by the atoms H1–C1–O1–C4, and the ψ dihedral angle is defined by the atoms C1–O1–C4–H4.

There are several different chromophores present in carbohydrates. Some of the biologically relevant polysaccharides have chromophores that absorb in the detectable regions observed for proteins, such as acyl groups, amides, and carboxylate functionalities found in uronic acids. These chromophores give rise to π→π* and n→π* electronic transitions. However, data analysis for polysaccharides is not analogous to proteins because of the differences in the monomer residues. A peptide amino acid monomer has a length of 0.36 nm, while 1,4-diequatorially linked pyranose rings have monomer residue lengths of 0.54 nm (Fig. 4).[3] The increased distance between chromophores does not allow for appreciable interactions; therefore, each monosaccharide unit is acting independently of one another. An exception to this scenario occurs in conformationally ordered polysaccharide chains, where interactions can occur between the chromophores provided that the proper orientation exists.[3] The presence of multiple chromophores, the lack of chromophore interactions, and the variety of monomer linkages combine to make CD analysis of carbohydrate secondary structure a very demanding task.

In addition to the difficulties encountered in the analysis of the CD data, the acquisition of such can also pose a challenge, since most chromophores present in common carbohydrates absorb outside of the range of commercially available CD instruments.[10] This is particularly apparent with unsubstituted carbohydrates, which only possess the hydroxyl, ring oxygen, and glycosidic oxygen functionalities. These functional groups give rise to higher energy, lower wavelength electronic transitions such as n→σ* and σ→σ*.[12] The n→σ* transition of the acetal oxygens at *C*-1 and *C*-5 is centered at approximately 175 nm, while the higher energy σ→σ* transition occurs at 150 nm. This last transition can only be investigated through the use of the very specialized technique of vacuum CD.[3]

CD has been utilized in the determination of linkage type and monosaccharide identification through the use of a chemical degradation technique, developed by Nakanishi and co-workers.[13] Their strategy involved the transformation of an oligosaccharide into a series of monosaccharides that were protected as bichromophoric derivatives. In their studies, the oligosaccharide was first peralkyl-bromobenzoylated.

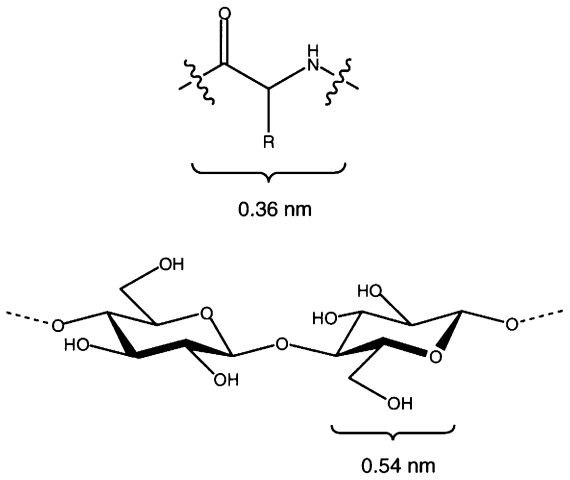


Fig. 4. Monomer length in a peptide versus 1→4 linked pyranose ring

The glycosidic linkages were subsequently cleaved under trifluoroacetolysis/bromination conditions to yield the anomeric bromides with the other linkage oxygens free, the trifluoroacetates having been lost on workup. The anomeric bromides were converted to the methyl glycosides using silver oxide ($Ag_2O$) in methanol. The final chemical modification step involved the introduction of a methoxycinnamoyl group. Fig. 5 illustrates this transformation. The choice of protecting groups was critical because bromobenzoates have a $\lambda_{max}$ of 245 nm, while methoxycinnamoyl groups have a $\lambda_{max}$ of 311 nm. These two chromophores could, therefore, be readily distinguished from each other, providing signature CD spectra based upon the linkage type and the monosaccharide present. The advantages of such a technique are that no synthetic standards are required for comparison because it is a spectroscopic technique, and that the chemical degradation/selective tagging sequences occur with high yields. Moreover, the amount of tagged monosaccharides necessary for analysis is in the nanomolar range. A disadvantage to this technique is that it is restricted to pyranoside sugars, as the more flexible furanosides present a more difficult calculational prospect.

The studies of monosaccharides by CD, even though they do not possess secondary structural features, provide invaluable information regarding the makeup of polysaccharides. Polysaccharides have also been investigated and these studies are distinguished by two primary classes, unsubstituted and substituted.[10] In the unsubstituted class, the carbohydrates do not bear functionalities other than hydroxyls, ring oxygens, and glycosidic oxygens. In the substituted class, additional chromophores are present, such as esters, amides, and acids, making the study of the latter class of molecules more accessible to commercial instrumentation. In order to study unsubstituted polysaccharides, one of two specialized methods needs to be employed; either vacuum CD or induced CD.

Induced CD is a technique whereby polysaccharides are complexed with achiral dyes to shift their chromophore absorbencies to wavelengths in the visible region of the electromagnetic spectrum. In one such study, Purdie and coworkers investigated the interaction between a series of dye molecules and oligomeric cellulose molecules (Fig. 6).[14] Several dyes were complexed with cellulose polymers, and also distinct oligomeric chain lengths, ranging from cellobiose ($n$=0) to cellooctaose ($n$=6). The results obtained in these studies substantiated the hypothesis that complexed oligosaccharides form helices in solution. The data from the induced CD study of the celluloses matched well with the vacuum CD data of the unsubstituted saccharides.[10] Furthermore, studies by Yalpani indicated the presence of right-handed helical structures for amylose (a polymer comprised of maltose units) in solution.[15] It was submitted that

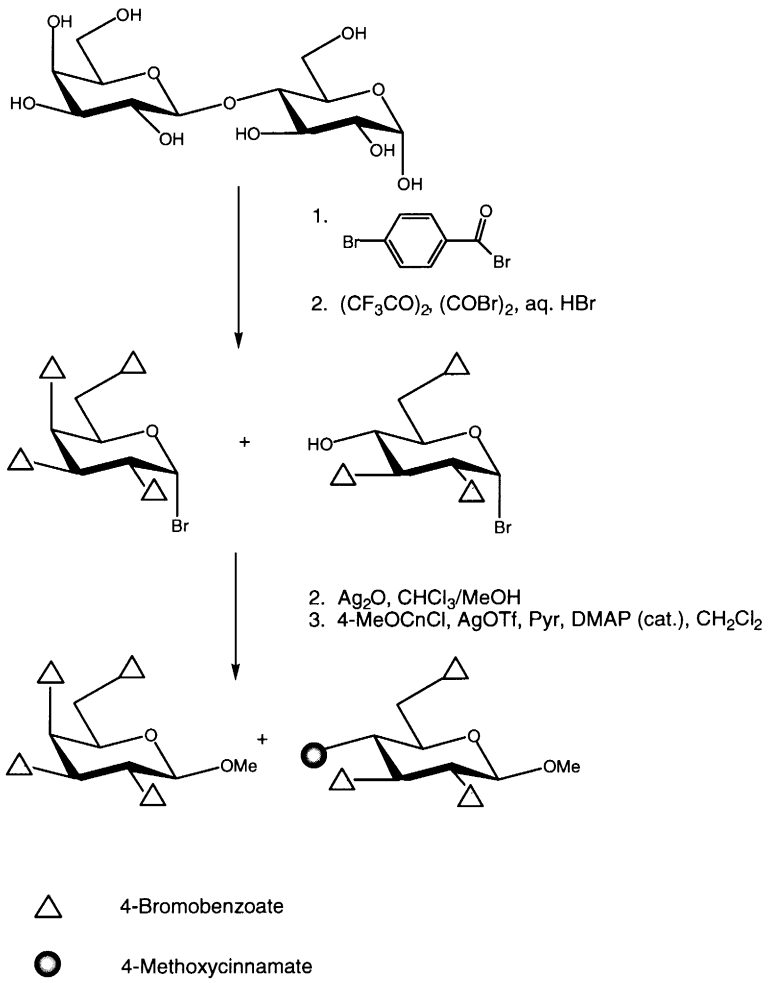


Fig. 5. The chemical degradation/selective chromophore tagging of oligosaccharides to determine the linkage and monosaccharide content by CD[13]

because the signs of the bands for the celluloses and the maltoses were opposite, they formed reverse-handed helices in solution. Cellulose and maltose differ in the conformation about the linkage between residues, with β 1→4 occurring in cellulose, and α 1→4 in maltose (Fig. 6). Therefore, since amylose adopts a right-handed helix, it was concluded that cellulose must form a left-handed helix.

The collection of CD data for polysaccharides with chromophores such as acids, esters, and amides is simplified because the absorbance of these chromophores is readily accessible by commercial instruments. However, the chromophores outside of the range of the commercial instruments, such as the hydroxyl, ring and glycosidic oxygens, may have an effect on the CD patterns seen for the amide and carboxyl transitions.[16] This adds further difficulties to the analysis of these molecules by CD. So, while the analysis of proteins has been developed to the point where common secondary structural features have been assigned a signature CD spectrum, and the calculations to determine the types of secondary features present have been reduced to standardized calculations, the same is not true of carbohydrate CD analysis. Each new molecule, or class of molecules, requires a unique way of analyzing the data.

Beyond the study of biologically relevant oligo- and polysaccharides, sophisticated conformational studies of carbohydrate interactions with peptides and enzymes, in addition to structural analyses of

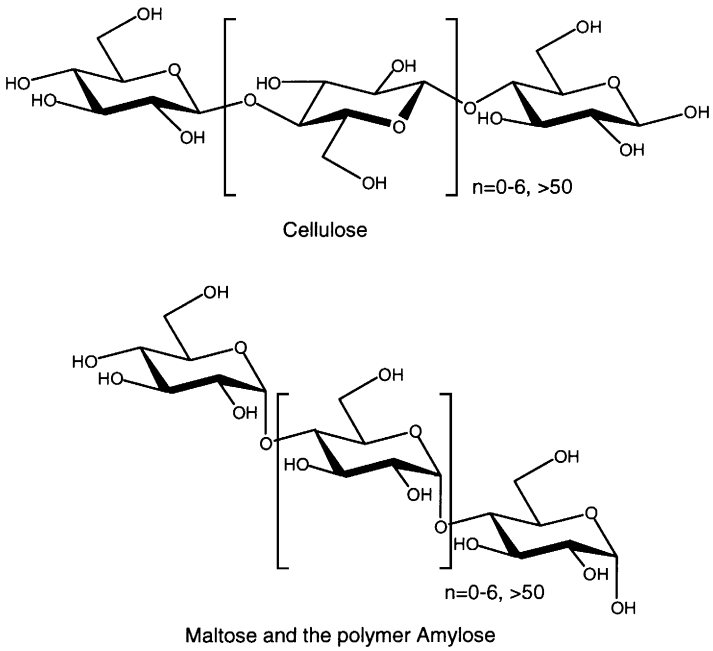


Fig. 6. The structures of cellulose and maltose. A polymer of maltose is known as amylose

bioconjugate molecules containing carbohydrates, have been employed in the past several years. These studies involve the use of circular dichroism in addition to other techniques, such as NMR spectroscopy and molecular modeling, to investigate the secondary structures of these complex biomolecules.

Fasman and associates used CD, NMR, and molecular dynamics to study the conformational properties of linear N-linked glycopeptides.[17] It was determined by molecular dynamics calculations and $^{1}H$–$^{1}H$ NOE NMR experiments that the conformation of the carbohydrate component of the N-linked glycopeptide was fixed in one conformation. This was followed by the finding that the carbohydrate constituent of the glycopeptide provided a constant CD that could be readily subtracted from the CD of the overall glycopeptide, yielding the CD of the peptide alone. Using this information, the investigators determined the ratios of two types of β-turn structures, type I and II, that predominated in various solvent systems, upon adding the CD contribution of the carbohydrate to that of the parent peptide. *N*-Glycosylation resulted in a decrease of the type I β-turn, with a subsequent increase in the percentage of the type II β-turn present. Molecular dynamics calculations were consistent with the CD results, with respect to the change in the ratio of β-turn structures.

The aforementioned study points to the need for supplemental information beyond CD to obtain more than qualitative information concerning the conformational properties of rather complex biomolecules. The combination of several different structure-determination techniques provides a powerful means with which to study conformational characteristics of increasingly complicated molecules.

## 3. The use of circular dichroism in defining the secondary structural characteristics of unnatural amide-linked molecules

The construction of unnatural amide-linked oligomeric materials with unique secondary structures for the purpose of mimicking biologically relevant structures represents a relatively new area of research. One long-term goal associated with this area of research is to synthesize molecules with defined

secondary structures for therapeutic purposes. Gellman has coined the term 'foldamers' to describe molecules having a strong tendency to adopt specific conformational patterns.[18] He has also outlined important criteria necessary for creating effective foldamers. First, backbones capable of forming appropriate structures must be defined. Second, the foldamers must have interesting and useful chemical functions inherent in their design, and third, the foldamers should be prepared in an efficient manner.

Gellman and coworkers have developed several interesting types of β-peptides. One is based on *trans*-2-aminocyclohexanecarboxylic acid (*trans*-ACHC), and another is based on *trans*-2-aminocyclopentanecarboxylic acid (*trans*-ACPC). The monomer unit and repeating unit structures are given in Fig. 7. The monomer units were selected based upon computational results that defined stable helical structures of oligomers composed of the monomers.[19] The helical structures predicted for the oligomers were a 14-helix for the *trans*-ACHC, and a 12-helix for the *trans*-ACPC. The 12- and 14-helices presented interesting hydrogen-bonding patterns. The models of the two oligomers predicted that the hydrogen bonds pointed in opposite directions between *trans*-ACHC and *trans*-ACPC, relative to the termini of the oligomers. This represents a unique situation that has not been reported for α-peptides.[18]

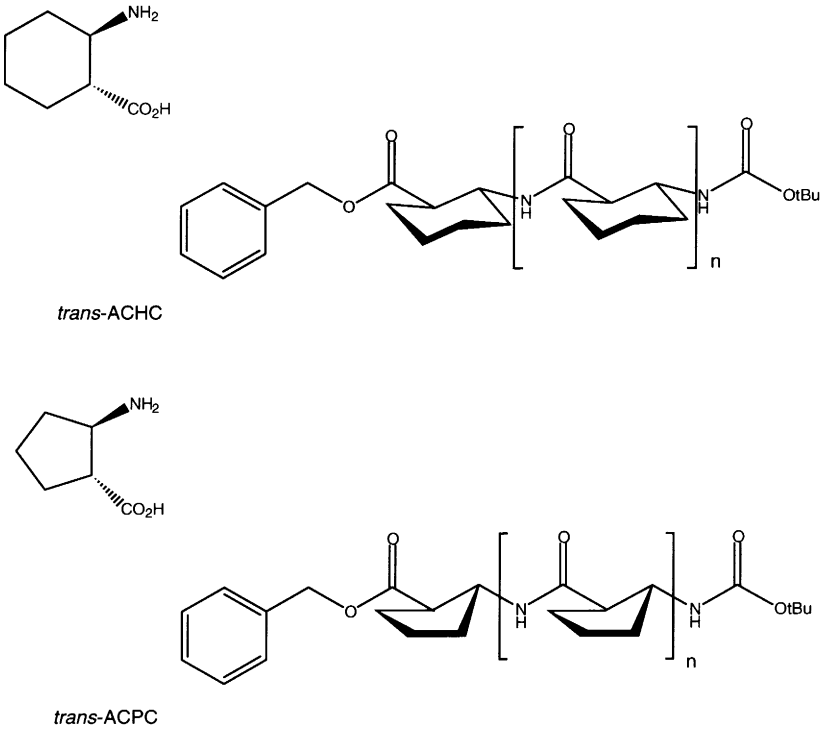


Fig. 7. Structures of monomeric and oligomeric *trans*-ACHC and *trans*-ACPC

Gellman and co-workers were able to obtain X-ray crystal structures of the tetramer and hexamer of the *trans*-ACHC, as well as the hexamer and octamer of the *trans*-ACPC molecules. The X-ray crystal structures showed that the calculationally predicted 14- and 12-helices for each type of oligomer were, in fact, correct.[19,20] Subsequent structural studies of these two oligomer classes by NH/ND exchange and CD further solidified the stability of the helical structures in solution. Gellman and co-workers noted that the CD signature spectrum generated for hexameric *trans*-ACPC differed from an acyclic 14-helix β-peptide. The acyclic peptide yielded a peak maximum at 197 nm, a zero-point crossover at ~207 nm, and a trough minimum at 215 nm. The *trans*-ACPC oligomer presented a different picture, with a maximum

at 204 nm, a zero-point crossover at ~214 nm, and a trough minimum at 221 nm. This suggested to the researchers that the cyclic β-peptide, *trans*-ACPC adopted a distinctive secondary structure.

Seebach and co-workers have also studied the secondary structural properties of β-peptides using circular dichroism. In one report, several water-soluble β-peptide derivatives were synthesized with phenylalanine, serine, and lysine β-amino acid analogs, as well as β-homophenylalanine.[21] The structure of one of the oligomers, a heptapeptide, composed of β-serine, β-alanine, and β-phenylalanine, is shown in Fig. 8. The CD of this molecule was measured in several different solvents including 2,2,2-trifluoroethanol, methanol, water, and buffered water at pH 3.6 and 11. A helix-specific trough was evident in each solvent at 215–220 nm and it was concluded that this CD band represented a $3_1$ helix. Another peptide containing β-homolysine did not display this CD band in buffered solution when compared to methanol, suggesting that a large number of cationic functionalities in close proximity may disrupt important hydrogen bonding patterns. Disruption of the helix did not occur in a heptapeptide composed of phenylalanine, alanine, and serine β-amino acids.

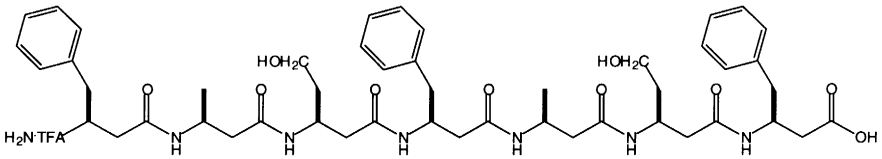


Fig. 8. Structure of a β-heptapeptide composed of the β-amino acids serine, phenylalanine, and alanine

The relative placement of the side chains was also shown to be critical for helix formation. Seebach ranked the β-amino acid components in the order of stabilization of a $3_1$ helix in water over methanol: $\beta^3$-Ser>$\beta^3$-Lys for polar residues in positions 3 and 6 of the peptide, and $\beta^2$-HHop>$\beta^3$-HHop=$\beta^3$-HPhe (HHop is homophenylalanine that has been homologated) for aromatic residues in positions 1, 4, and 7. The information generated in this study could be useful for the design of combinatorial β-peptide libraries with specific $3_1$-helical properties.

Seebach and co-workers further probed the effect of temperature on β-peptides in a $3_{14}$-helical conformation in methanol both by NMR and CD.[22] It is well-known that proteins with secondary structures denature at high temperatures. The same is true for peptides composed of α-amino acids.[22] The denaturing process is also called cooperative unfolding. A study was undertaken to determine whether or not the cooperative unfolding process occurred in peptides composed of β-amino acids. A heptapeptide composed of the β-amino acid analogs of alanine, valine, and leucine was studied (Fig. 9). It was assigned a $3_{14}$-helical secondary structure, based upon NMR data and molecular dynamics simulations. Using an NH/ND exchange experiment in $CD_3OH$, the investigators determined that the half-lives for the amide protons were large, ranging from 5 to 262 min. The molecular dynamics revealed a 'melting point' of 340 K, where both the folded and unfolded peptide microstates were equally populated. The heptapeptide also showed reversible protein folding in the molecular dynamics simulation, something that had not been previously observed.[23]

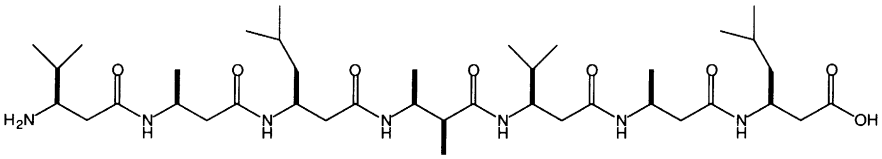


Fig. 9. A heptapeptide composed of the β-amino acids alanine, valine, and leucine

Temperature-dependence of the heptapeptide structure was assessed using NMR and CD. The spectra were recorded in 10 K increments from 293 to 353 K. The *J* coupling constants for the NH and C(β)-

H protons were measured and compared at each temperature. The *J* values decreased only slightly with increasing temperatures, and the $3_{14}$-helix was still intact at 353 K. However, the *J* value for the end residues did decrease (by 0.7 Hz) more than the internal residues (0.4 Hz) suggesting that higher temperatures promoted fraying. The CD studies at three different temperatures, 293, 313, and 333 K, mirrored the results obtained by NMR. The assigned $3_{14}$-helical CD signature spectrum with a strong maximum at 198, and an intense minimum at 215 nm, was evident at all three temperatures. Both the NMR and CD results, therefore, indicated that unlike α-amino acid-based compounds that denature at higher temperatures, β-peptides have an increased stability at elevated temperatures.

Both Seebach and Hanessian have reported the synthesis and secondary structural characteristics of γ-peptides.[24,25] Seebach and co-workers investigated the secondary structure of a γ-hexapeptide composed of the γ-amino acid analogs of L-valine, L-alanine, and L-leucine by solution phase NMR. These studies showed that the γ-hexapeptide adopted a stable right-handed helix.[24] Hanessian and co-workers synthesized a series of γ-peptides by homologation of L-alanine and L-valine.[25] They used a combination of NMR, molecular dynamics, and CD to determine the secondary structural characteristics of tetramers, hexamers, and octamers. Fig. 10 gives the representative structure of a tetramer used in the studies. The two-dimensional NMR studies yielded NOE (nuclear Overhauser effect) data, that when subjected to molecular dynamics yielded a right-handed helical structure with a pitch of 5 Å and hydrogen bonding patterns forming 14-membered rings. Variable temperature NMR experiments were also performed on these molecules, much like those of Seebach, to probe the stability of the helix. The experiments were performed over a range of 273–323 K. The chemical shifts of the inner residue NH protons were only mildly affected by temperature changes, again pointing to the stability of the helix. Not unexpectedly, the CD measurements in this study did not give the same characteristic patterns as those of either the α- or β-peptide classes. More experiments with these unusual peptides are required before signature CD spectra can be identified.

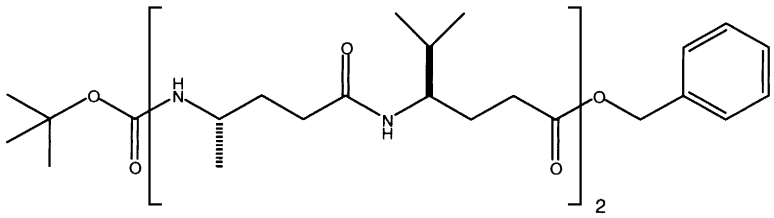


Fig. 10. Structure of a tetrameric γ-peptide

The results presented thus far on the structural features of the unnatural peptide compounds indicate that these molecules possess thermodynamic stability that exceeds that of naturally occurring peptides. Furthermore, it has been reported that β-peptides are resistant to cleavage by natural proteases.[22] These two properties of unnatural peptides make them excellent candidates for incorporating into novel drug design constructs.

## 4. Use of circular dichroism to define secondary structures of sialic acid-containing oligomers

*N*-Acetyl neuraminic acid (NeuAc) is a naturally occurring carbohydrate that is expressed in living organisms from microbes, such as *Escherichia coli*, to humans (Fig. 11). It is the most abundant member of a class of compounds known as the sialic acids, and often, the name sialic acid is used synonymously with NeuAc. NeuAc can also be classified as a δ-amino acid based upon the presence of both a carboxylic acid and a protected amine functionality.[26] NeuAc, and the oligomeric and polymeric natural products

derived from it, have been studied extensively by our research group, as well as many others. Circular dichroism has been a powerful tool used to evaluate the chromophore signature bands, and to investigate the secondary structures of oligo- and polysaccharides derived from the sialic acid skeleton.

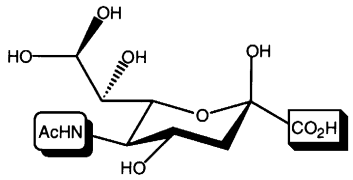


Fig. 11. *N*-Acetyl neuraminic acid, a natural δ-amino acid

CD spectra for both the α- and β-glycosides of NeuAc were reported by Morris and co-workers in 1979.[27] They also measured the CD of the reduced β-anomer to determine the contribution of the carboxylic acid to the CD pattern (Fig. 12). From the CD of these three compounds, the investigators arrived at important conclusions concerning the relationship of the chromophore and the observed CD signal. First, the main CD band, centered below 200 nm was attributed to the acetamido group, and it showed minimal sensitivity to functionality changes or the anomeric configuration. Second, a trough at approximately 225 nm was assigned to the n→π* transition of the carboxy chromophore because of its absence in the reduced molecule. They further determined that the α-glycosides of sialic acid gave rise to a negative band at 225 nm, while β-glycosides gave a positive band. Restricting the flexibility about the glycosidic bond was found to increase the magnitude of this band.

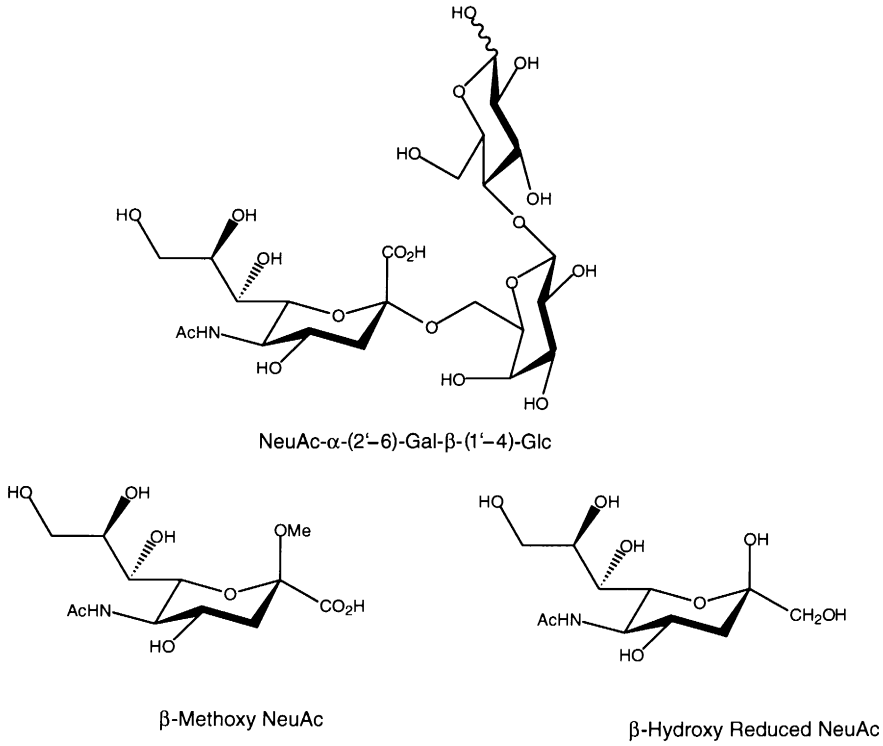


Fig. 12. Structures of three NeuAc derivatives investigated by CD. The α-anomer is composed of NeuAc linked α 2→6 to a lactosyl moiety. The β-anomer is the methyl glycoside, and the reduced NeuAc is also in the β-configuration with an unprotected anomeric hydroxyl

In addition to evaluating CD patterns to determine the effect of the anomeric configuration, a predictive tool for NeuAc and its simple glycosides was proposed by Listowsky and associates.[28] The planar rule can be used to evaluate the spatial distribution of pendant groups about the chromophore. This allows for the correlation of the sign of the observed Cotton effect in the CD with the geometric pattern of the molecule.[27] Fig. 13 illustrates the predictive properties of the planar rule for sialic acid. This rule provides a simple means by which the sign of the n→π* transitions can be predicted, based upon which side of the chromophore the other parts of the molecules lie on. Fig. 13 illustrates the prediction of a positive band for β glycosides of NeuAc, and a negative band for the α glycosides. The two different conformations seen for each anomer, with either the ring or glycosidic oxygens eclipsed, predict the same CD band sign. Morris and co-workers evaluated the validity of the planar rule using a series of fused lactone molecules, and found it to match the CD data.[27]

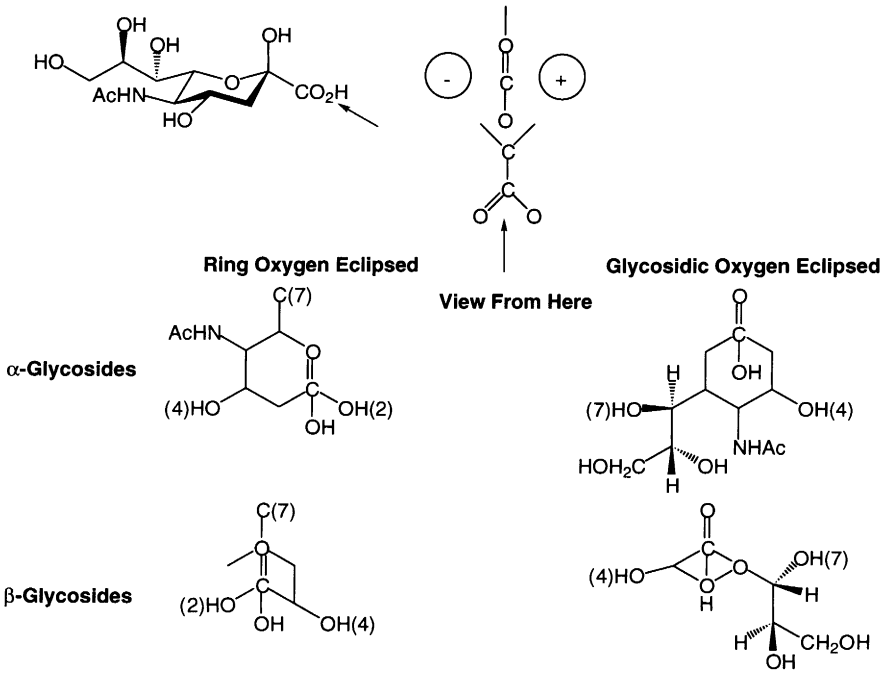


Fig. 13. The planar rule for NeuAc. The planar rule can be used to evaluate the spatial distribution of pendant groups about the chromophore, and ultimately correlate the observed Cotton effect in the CD with the geometry of the molecule[27]

Building on the conformational and structural knowledge for the sialic acid monomer, many studies have been undertaken to understand biopolymers composed of multiple NeuAc residues in oligomeric and polymeric forms. Of particular interest to our research is the study of colominic acid, an α 2→8-linked homopolymer of NeuAc. Colominic acid is a capsular polysaccharide of the pathogenic bacterial strain *E. coli* K-235. The structure of colominic acid is identical to the capsular polysaccharides of other pathogenic bacteria, *Neisseria meningitidis* serogroup B, and *E. coli* K-1 (Fig. 14).[29–31] These bacteria are the causative agents in cerebrospinal meningitis, a disease manifested in infants and young children, as well as some immunocompromised individuals.

Colominic acid is generated in these bacteria through a series of biosynthetic steps (Fig. 15). In the first step, NeuAc is generated from *N*-acetylmannosamine and pyruvate by the enzyme Neu5Ac synthase.[31] The next step involves the activation of NeuAc to CMP-NeuAc (CMP is cytidine monophosphate) by the enzyme, CMP-Neu5Ac synthetase.[31,32] The last step in the biosynthetic pathway involves the synthesis of the colominic acid polymer by a polysialyltransferase complex.[33,34] The synthesis of colominic acid

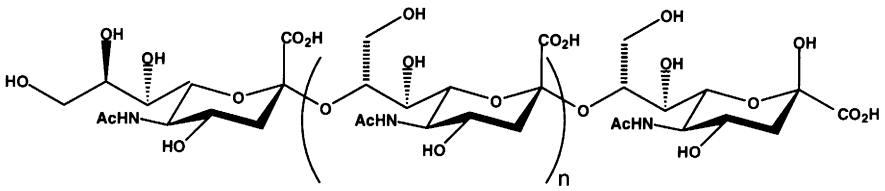


Fig. 14. The structure of colominic acid

begins with the transfer of CMP-NeuAc to the lipid undecaprenyl phosphate.[35] Additional NeuAc residues are transferred to the non-reducing end of the growing chain, and finally translocated to the outer membrane.[36]

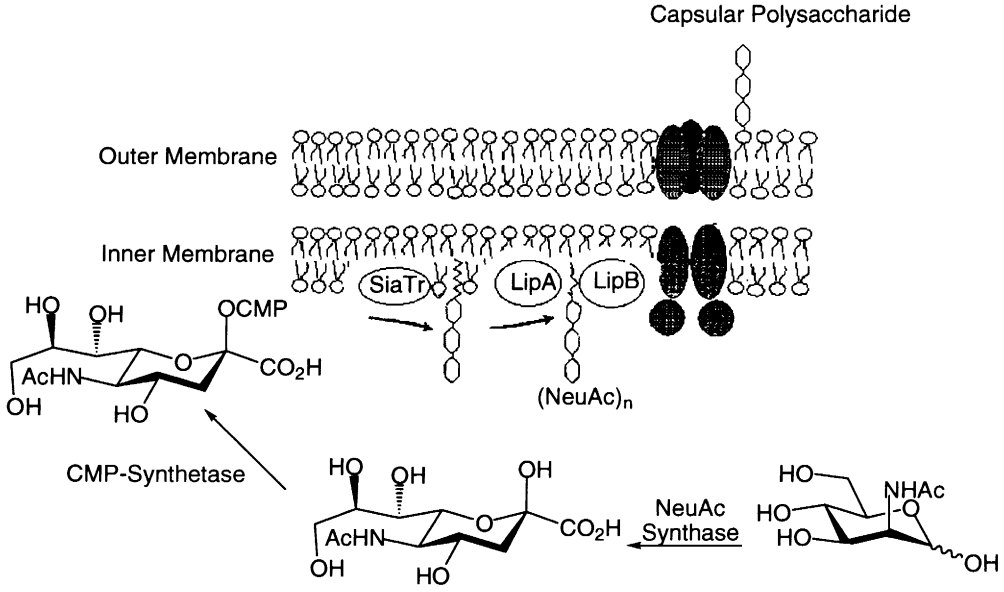


Fig. 15. The biosynthetic pathway for the production of colominic acid in bacteria

In *E. coli* K-235, colominic acid is released from the surface of the bacteria when bacterial growth ceases showing kinetics that are typical of a secondary metabolite.[37] The length of colominic acid obtained is a function of pH.[34] However, the purified polysaccharide can be cleaved into discrete oligomers utilizing a method reported by Roy and Pon in 1990.[38]

Structural studies of colominic acid and the identical polysaccharide generated by *N. meningitidis* serogroup B were undertaken by several groups, beginning in the early 1980s. NMR and computational methods were used to facilitate conformational studies directed at identifying the epitope of *N. meningitidis* serogroup B polysaccharide. It had already been determined that the serogroup C polysaccharide (Fig. 16) from the same organism was immunogenic, meaning that immunization with the group C polysaccharide led to the formation of protective antibodies against the bacterium. However, the same was not true of the serogroup B polysaccharide.[39] Several hypotheses were submitted to explain the poor immunogenicity of the group B polysaccharide; namely the sensitivity of the polysaccharide to cleavage by neuraminidases, cross-reactivity with 'self' antigens,[40] and the intrinsic 'floppiness' of the type B polysaccharide.[41] Sela proposed that there may be an inherent difference in the epitope recognized by the antibodies. Specifically, that the group C polysaccharide presents a linear epitope for antibody binding, while the group B polysaccharide has a conformational epitope recognized by the antibody. The binding

of the antibody to the group B polysaccharide, therefore, would be dependent on the three-dimensional structure of the antigen.[42]

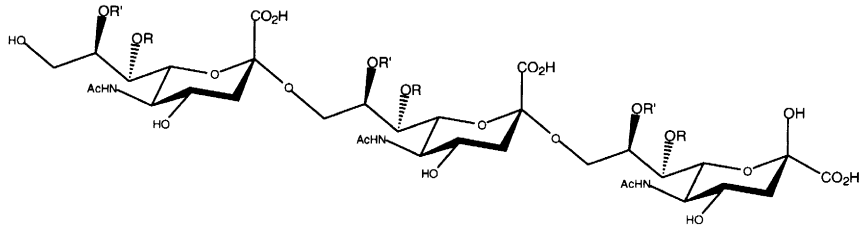


α-(2'–9)-*N*-Acetyl and *O*-Acetyl Neuraminic Acid Type C

R = R' = H
R = R' = $COCH_3$
R = H, R' = $COCH_3$
R = $COCH_3$, R' = H

Fig. 16. Structure of the serogroup C polysaccharide of *N. meningitidis*

Lifely and co-workers were the first to investigate the differences in the conformation between the group B and C polysaccharides of *N. meningitidis*, using a combination of NMR and computational techniques.[39] They concluded from their results that the B polysaccharide had little internal flexibility, and a different three-dimensional structure from the C polysaccharide. This was based on the C polysaccharide having internal or segmental motion in the C-7 to C-9 side chain of the repeating unit. The B polysaccharide, on the other hand, had little or no such movement, and tumbled in solution as a rigid species, with rotation only possible about the C-9 pendant group.

Jennings and co-workers further investigated the antibody binding epitope of the group B meningococcal polysaccharide (GBMP). Using a meningococcal group B-specific horse antiserum, the epitope chain length in the polysaccharide was determined by evaluating the antibody-binding capabilities of discrete chain length oligosaccharides.[43] The experiment involved first binding a polymer of $^3$H-labeled GBMP to the horse antibody, and then counting the $^3$H signal with a scintillation counter. Next, oligomers of known chain length were introduced to the mixture as inhibitors of the antibody–antigen interaction. The $^3$H signal was again counted for each inhibitor and the % inhibition was determined. Through this experiment, they were able to determine that displacement of the labelled polysaccharide was only achieved with a critical chain length of 10 NeuAc residues. This was an unusual result, as carbohydrate epitopes for antibody binding generally require only six to seven linearly arrayed sugar residues to achieve strong binding.[44] After an extended conformation for antibody binding to GBMP had been identified, NMR studies were undertaken to further characterize this unusually long epitope.[45] Two-dimensional NMR experiments were performed to determine the solution phase properties of a decasaccharide of colominic acid. These studies showed that the two terminal disaccharides on either end of the oligosaccharide had different conformations than the inner residues, as evidenced by differences in chemical shifts and in the *J* coupling values. Jennings and co-workers concluded that the antibody recognized the inner six residues of the decamer, and that this binding was conformationally driven.

Jennings and co-workers, and independently Yamasaki and Bacon, performed additional NMR experiments and computational studies to arrive at similar helical structures for GBMP.[46,47] Yamasaki and Bacon performed DQF-COSY and pure absorption 2D NOE NMR with three mixing times, then utilized the NOE data to perform calculations using CORMA (complete relaxation matrix analysis). Their analysis suggested a helical conformation for the GBMP with $\phi$ angles of $-60$–$0°$, $\psi$ 115–175°, or $\phi$ 90–120°, and $\psi$ 55–175°. Fig. 17 illustrates the positioning of the $\phi,\psi$ angles in GBMP. Other secondary

structural features of GBMP identified by Yamasaki and Bacon was a repeating unit incorporating 3–4 residues per turn, and a pitch of 9–11 Å.

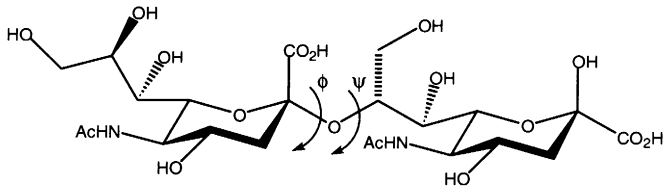


Fig. 17. ϕ, ψ Angles in polysialic acid. A dimer is shown for clarity. The ϕ dihedral angle is defined by the atoms O6–C2–O8–C8, and the ψ dihedral angle is defined by the atoms C2–O8–C8–C7

Jennings and associates also performed 2D NOE NMR experiments in addition to potential energy calculations. While their results did not yield specific structures that fit all of the collected data, some possible conformations of the polymer were proposed, and they concluded that the polymer was composed of a random coil structure with local regions of helicity. Moreover, the negatively charged carboxylate residues were shown to be critical for stability of the helical conformation.[48]

Jennings and co-workers also solved the X-ray crystal structure (2.8 Å resolution) of an antibody binding fragment specific for the α (2→8)-polyNeuAc chain.[49] They overlaid the crystal structure with several different proposed oligosaccharide helical structures to determine the best overlap interactions between the antibody binding fragment and the oligosaccharide. In doing so, they were able to better characterize the helical properties of polyNeuAc when bound to a specific antibody and a helix with six residues per turn, and a pitch of 36 Å was optimal.

Circular dichroism has been utilized to further elaborate the structure of α (2→8)-linked polyNeuAc. In 1994, Inoue and co-workers studied the $Ca^{+2}$ binding properties of colominic acid using equilibrium dialysis and CD.[50] In the equilibrium dialysis experiments, three molecular weight ranges of colominic acid were used, a high-molecular weight polymer (H-CA) with a degree of polymerization (DP) of 24, a medium-molecular weight oligomer (M-CA) with a DP of 15, and a low molecular weight oligomer (L-CA) with an average DP of 4.8. $^{45}Ca$ was used as a tracer. The investigators determined that the binding of calcium to colominic acid occurred in a biphasic manner, with a high affinity binding and a low affinity binding strength. This suggested that two different types of complexation were occurring between the oligomers and the cation. The binding constants for the high affinity binding event were in the range of $1–10\times10^3$ $M^{-1}$, while the low affinity binding had $K_a$ values of approximately 200 $M^{-1}$. The binding constants for colominic acid were significantly higher than that of NeuAc, which was 121 $M^{-1}$.[51] The higher affinity sites in colominic acid had several binding sites for calcium, versus one in sialic acid, which indicated that the calcium binding mode was different in the oligo- and polysaccharide compared to the monomer. Scatchard analysis was used to not only estimate the binding constants, but also the approximate number, *n*, of calcium ions that bound per number of sialic acid residues. For the high affinity binding event, it was determined that both the high- and medium-molecular weight colominic acids were able to bind about one calcium ion per every three NeuAc residues. The low molecular weight colominic acid was only able to complex one calcium ion for every five residues of NeuAc. In the low affinity binding event, only one calcium ion was able to bind both the oligomeric and polymeric colominic acid. Table 1 summarizes the equilibrium dialysis results.

The CD of colominic acid in the presence of $Ca^{+2}$ was also recorded.[50] While no change in the negative band centered at 225 nm was noted upon addition of calcium, a measurable decrease in ellipticity was seen in the positive band at ~195 nm. The changes were attributed to an alteration in the interresidue interactions leading to significant changes in the conformation of colominic acid upon binding calcium. Another aspect of the CD investigation involved the measurement of $Ca^{+2}$-induced changes in ellipticity,

Table 1
Equilibrium binding results for calcium complexation with colominic acid of varying lengths

| Calcium Binding to Colominic Acid | DP | Ka (M-1) | n (mol/mol) |
|---|---|---|---|
| High-Affinity Binding | | | |
| H-CA | 24 | 1.39E+04 | 0.30 |
| M-CA | 15 | 1.49E+04 | 0.29 |
| L-CA | 4.8 | 6.45E+03 | 0.21 |
| Low-Affinity Binding | | | |
| H-CA | 24 | 2.08E+02 | 0.82 |
| M-CA | 15 | 2.21E+02 | 0.88 |
| L-CA | 4.8 | 2.29E+02 | 0.80 |
| Calcium Binding to Colominic Acid in the Presence of 0.11 M NaCl | | | |
| High-Affinity Binding | | | |
| M-CA | 15 | 6.79E+02 | 0.19 |
| L-CA | 4.8 | 7.08E+02 | 0.20 |
| Low-Affinity Binding | | | |
| M-CA | 15 | 4.40E+01 | 1.30 |
| L-CA | 4.8 | 4.01E+01 | 1.80 |

represented as a function of ion concentration, both in the absence and presence of 0.11 M NaCl. The binding profile of colominic acid to $Mg^{+2}$ was also investigated by CD. The authors concluded that colominic acid had different binding affinities for individual cations, and that the induced conformational change in colominic acid was specific for mineral cations. $Ca^{+2}$ had the highest affinity for colominic acid, compared to $Na^{+}$ and $Mg^{+2}$.

Recently, Bystricky and associates reported a comprehensive study of the physical properties of colominic acid using circular dichroism.[52] The CD spectra of the sodium salt of colominic acid and the *N*-deacetylated polymer were compared at two different temperatures, 5 and 70°C. The *N*-deacetylated polysaccharide was studied to determine the contribution of the carboxyl chromophore $n \rightarrow \pi^*$ transition ranging from 205 to 225 nm, as the *N*-acetyl and the carboxyl chromophore bands for this transition overlap. It was found that the large positive band centered on 200 nm in the natural colominic acid was due to the *N*-acetyl chromophore, because the *N*-deacetylated polymer has a negative band in this region. Furthermore, no significant contribution to the CD spectrum at two different temperatures was detected. Another experiment evaluated the effect of ion complexation to both polymers, similar to the study of colominic acid complexation carried out by Inoue and co-workers.[50] While the CD spectra for colominic acid complexed with the same three counterions, $Na^{+}$, $Ca^{+2}$, and $Mg^{+2}$, looked similar to that of Inoue et al., the conclusions drawn were different. Bystricky and co-workers concluded that since there was no great change in the CD of colominic acid over different concentrations of salt (NaCl was tested from 0.04 to 1.0 M), there could be no possibility of a cooperative order-to-disorder transition, as occurs in the helix-coil case, under either temperature- or salt-induced circumstances. They did not rule out the possibility of the existence of several different local helices with a different number of residues per turn but similar energies that portray helical transitions. The CD for the *N*-deacetylated polysaccharide in the presence of different counterions was even less sensitive to changes in the conformation.

Bystricky and co-workers went on to study the CD of discrete oligomers of colominic acid. They isolated oligosaccharides ranging from 2 to 17 residues, and recorded the CD of each. They assigned the first negative band at approximately 220 nm to the chiral environment of the C′1 carboxyl group in the vicinity of the glycosidic bond. This band increased in intensity up to $n$=9 residues, beyond which the molar ellipticity remained constant. They concluded from their results that the CD for the shorter oligomers ($n$=2–8) varied significantly, and when the oligomer length reached $n$=9, some stability in

the secondary structure was attained. This is consistent with Jennings and co-workers' findings that a decamer was required to achieve a stable epitope conformation.[45,49]

We have also studied the secondary structural characteristics of colominic acid oligomers by circular dichroism, for the purpose of gaining a better understanding of their conformational attributes. Knowledge gained from such studies will promote the development of effective vaccines against bacterial infections by organisms such as *N. meningitidis* type B. The polyanionic character and proposed helical structure of the polysaccharide have also made it a candidate as an entry mechanism inhibitor in HIV. Sulfated colominic acid has shown in vitro activity against the virus, through polyanionic binding to the V3 loop.[53] The possibility also exists for colominic acid and its derivatives to bind the known helical CD4 binding site of gp120. Therefore, further investigation of the colominic acid polysaccharide, oligomers, and derivatives using the technique of circular dichroism is merited.

As mentioned earlier, colominic acid may be produced through the growth and bioprocessing of *E. coli* K-235, where at the late logarithmic growth phase the bacteria shed the polysaccharide coat into the fermentation broth as a secondary metabolite.[37] The fermentation broth is then isolated by centrifugation and subsequent filtration. Ethanol precipitation is generally used as the first purification technique, followed by dialysis.[54] The colominic acid polymer may be further purified through precipitation first with streptomycin sulfate, followed by hexadecyltrimethylammonium bromide.[55] Colominic acid can also be purchased in very pure form from a few sources, such as Sigma and Nacalai Tesque.

The pure colominic acid polymer was hydrolyzed into discrete chain lengths using the procedure of Roy and Pon.[38] The production of specific oligomers was optimized by altering the time, temperature, and pH at which the hydrolysis progressed. The freeze-dried hydrosylate was then purified using size exclusion chromatography to yield the individual oligomers in pure form. Generally, baseline separation of these oligomers was only achieved for approximately monomer through tetramer, after which overlapping of the eluting peaks occurred. The oligomers were further purified by subjecting them individually to the same size exclusion column. The purity was confirmed using electrospray mass spectroscopy in the negative ion mode ($ESI^-$), as it clearly showed the different charge states of the oligomers present, when evaluated by the equation presented in Fig. 18. The presence of any interfering oligomers is easily detected by this method. ESI mass spectrometry has the added benefit of being free of matrix peaks that occur with fast atom bombardment mass spectroscopy (FABMS). Others have utilized colorimetric techniques such as the resorcinol method developed by Svennerholm to determine the chain lengths of the isolated oligomers.[56] We found this method to be very time consuming, and the results too qualitative to be of value.

$$\mathbf{(M/Z) = (M - H)/Z}$$

Fig. 18. Equation for the determination of the charge states of polyanionic molecules in electrospray mass spectroscopy, negative mode. M is the molecular weight of the molecule, Z is the charge, and H is the number of deprotonated protons on the molecule

Circular dichroism was performed on the monomer NeuAc, oligomers ranging from dimer to nonamer, and on the commercially available polymer, colominic acid. The CD for each molecule was measured in 50 mM phosphate-buffered water at pH 4.0. Fig. 19 shows the CD spectra of colominic acid and its oligomers. We have taken into account the contribution of chromophores for each oligomer by dividing the molar ellipticity values at each wavelength by the number of residues per molecule. In doing so, the relative contributions made to the CD by each oligomer can be evaluated. In some cases, the addition of one more residue imparts greater molar ellipticity to the oligomer because of the formation of a stable secondary conformation, and in other cases it does not. In other words, the additivity of residues to the secondary structure is not a linear process, and depends greatly upon the stability of the conformations achieved.

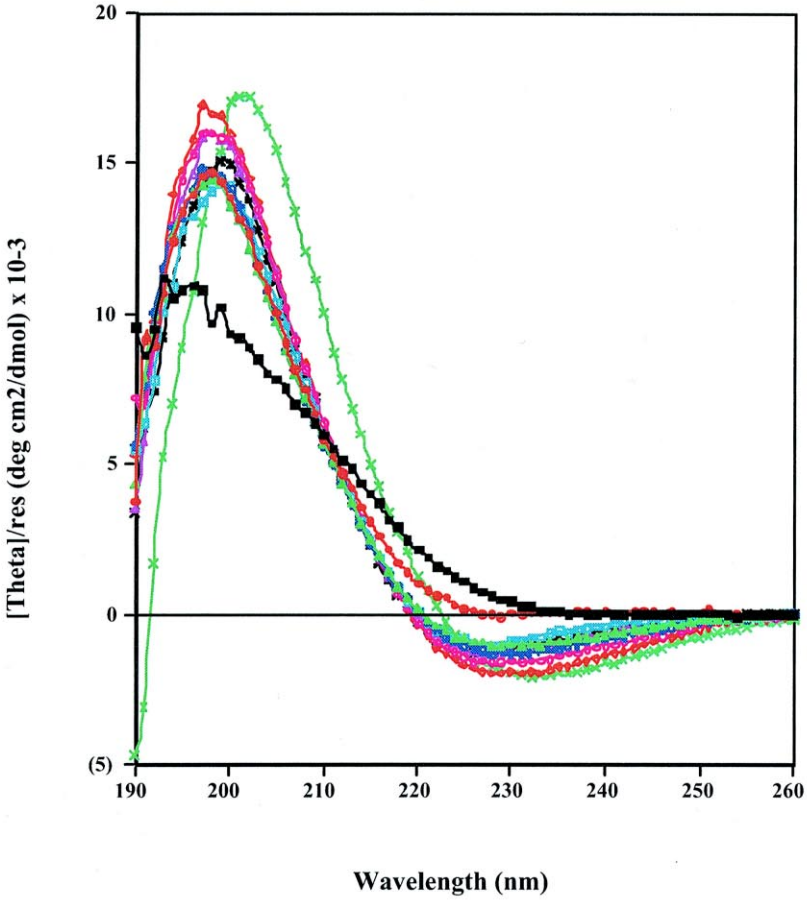


| | Chain Length | Peak Max | Trough Min | Peak - Trough |
|---|---|---|---|---|
| ■ | Monomer | 10.260 | 0.498 | 9.762 |
| ● | Dimer | 14.745 | -0.009 | 14.754 |
| ▲ | Trimer | 14.460 | -1.037 | 15.497 |
| + | Tetramer | 14.830 | -1.327 | 16.157 |
| ❑ | Pentamer | 14.379 | -0.942 | 15.321 |
| ○ | Hexamer | 16.022 | -1.602 | 17.624 |
| Δ | Heptamer | 16.006 | -1.286 | 17.292 |
| ✳ | Octamer | 15.095 | -1.309 | 16.404 |
| ◆ | Nonamer | 16.968 | -1.974 | 18.942 |
| x | Polymer | 17.2130 | -2.0900 | 19.303 |

Fig. 19. CD spectra of NeuAc, dimer through nonomer of colominic acid, and polymeric colominic acid. The table shows the peak–trough analysis for the constituent oligo- and polysaccharides. The units for all numerical values are (deg $cm^2$/dmol)$\times 10^{-3}$

Our CD spectra match those of Bystricky and co-workers, with the n→π* *N*-acetyl transition centered at approximately 198 nm, and the higher wavelength n→π* negative band at approximately 225 nm.[52] Interestingly, the spectrum for the colominic acid polymer ($n$~100 residues) is red-shifted in the low wavelength band by approximately 4 to 202 nm. This may be due to the presence of coiled interactions in the polymer that are not present in shorter oligomers. The table in Fig. 19 contains the legend and peak-to-trough analysis. The peak-to-trough (P–T) ratio can be a useful means for evaluating the ellipticity profiles within a class of related molecules.[57] Morris and co-workers used this technique to study the alginate polymer, and by doing so were able to measure the relative quantities of constituent monosaccharides within the heteropolysaccharide.

For our purposes, the P–T analysis was used to qualify the oligosaccharide conformational changes in varying chain lengths. In looking at the ratios directly, one notes the gradual increase from the monomer to the tetramer, then a decrease in the pentamer. The short oligomers are very flexible and, therefore, would be expected to have many different conformations. Perhaps the pentamer is an oligomer that is long enough to begin to have certain conformations that occur in greater frequency than the shorter oligomers, which would explain the decrease in ellipticity that is seen for this particular chain length. Both the hexamer and heptamer have approximately equal P–T ratios that are larger in value than the pentamer. This suggests that these oligomers may adopt the same types of conformations in solution, because the values are so similar in magnitude. Again at the octamer stage, a decrease in the P–T ratio signals a change in structural conformation. The nonamer ratio again increases, and is approaching the P–T ratio of the polymer. The nonamer is the most likely oligomer chain length to adopt a helical structure based upon the NMR and computational results already discussed, because it is long enough to have six internal residues capable of hydrogen bonding properly.

In addition to the polyanionic form of colominic acid, another more structurally constrained derivative exists. Colominic acid is capable of forming interresidue six-membered lactone rings in acidic environments (Fig. 20). Lifely and co-workers first reported lactone ring formation in the polysaccharide in 1981.[58] The degree of esterification that occurred between the pH values of 3.0 and 6.0 ranged from 53 to 2.5%, respectively, in the group B polysaccharide. The formation of lactone rings could be achieved under several conditions, from acidic aqueous solutions, to hydrofluoric acid, carbodiimide, or glacial acetic acid treatments. Using an immunoprecipitation reaction, Lifely and co-workers showed that as little as 9% lactonization of the polysaccharide was sufficient to completely abolish recognition of the open chain polymer by the antibody. This finding has significant implications in the pathology of bacterial meningitis caused by *N. meningitidis* and *E. coli* K1. The possibility of negative charge density control through lactonization by these organisms in vivo may explain their ability to escape recognition by the immune system.

Several groups have studied the lactonization process using CD. In 1980, Gekko evaluated solvent effects on the CD of polymeric colominic acid.[59] CD spectra of colominic acid were recorded at six different pHs: 2, 3, 4, 5.5, 8, and 10. Gekko noted that there were significant differences in the polymer CD pattern in acidic versus basic media. Colominic acid had a negative band shift to 235 nm at lower pH values, and had a crossover point at 207 nm, and a positive band at 197 nm. The sodium salt forms (higher pH) had a negative band centered at 228 nm, with the subsequent shift of the crossover point and positive band to longer wavelengths, compared to the polymer under acidic conditions. Furthermore, under basic conditions the ellipticities were diminished in comparison with acidic conditions. The positive band in the colominic acid CD was not as sensitive to changes in the pH of the solution, as evidenced by the smaller shifts in wavelength in acidic and basic solutions. The positive band compared well with both the acid and sodium salt forms of sialic acid, and it was assigned to the same carboxyl n→π* and amide n→π* and π→π* transitions as the monomer. The negative band could not be assigned based on Gekko's

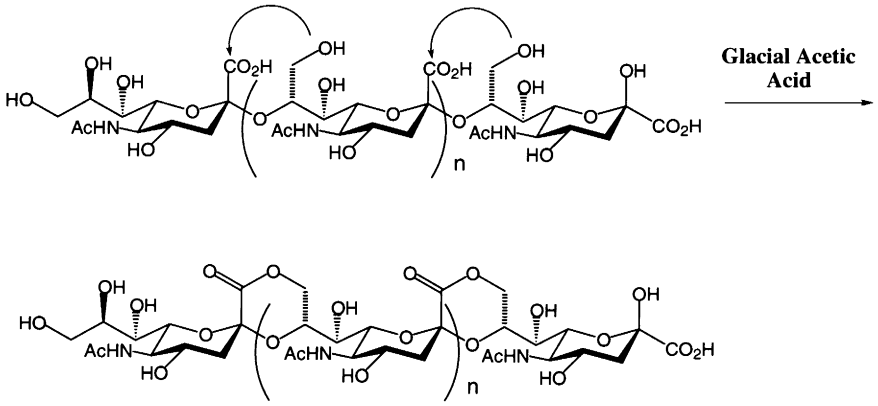


Fig. 20. Formation of interresidue lactone rings in colominic acid treated with acid

results. Crescenzi and associates also studied colominic acid at different pH values, and achieved similar results.[60]

Terabayashi and co-workers reported a study of the lactonization process in oligomers of colominic acid in 1996.[61] In this study, a tetramer of colominic acid was monitored by CD in the presence of 10 mM HCl. They found that the negative band at 228 nm shifted to the higher wavelength of 235 nm, with time, and also that the ellipticity values increased with time. They also evaluated the lactonization of the dimer, trimer, pentamer, and decamer of colominic acid by CD and reported the ellipticity values with the number of residues taken into account (Table 2). They determined that the molar ellipticity/residue, $[\theta_R]$, ranged from ~1.45 to $1.55\times10^4$ (deg cm$^2$)/dmol, and that the molar ellipticity, $[\theta]$, was additive with respect to the number of lactone rings.

Table 2
Molar ellipticity of NeuAc oligomers at 235 nm. $[\theta]$ is the molar ellipticity at 235 nm in the units of $10^4$ (deg cm$^2$)/dmol. $[\theta_R]$ is the molar ellipticity per residue in the same units

| | Dimer | Trimer | Tetramer | Pentamer | Decamer |
|---|---|---|---|---|---|
| $[\theta]$ | 1.47 | 2.88 | 4.65 | 5.84 | 13.68 |
| $[\theta_R]$ | 1.47 | 1.44 | 1.55 | 1.46 | 1.52 |

While the general characteristics of the CD for the oligolactones of colominic acid have been well-studied, assignment of the secondary structures of this more highly constrained class of molecules has not yet been achieved.

In addition to the naturally occurring α (2→8)-glycosidically linked colominic acid oligomers, and the related oligolactones, we have synthesized a novel class of β-methyl glycoside amide-linked sialooligomers. The structures of these novel compounds appear in Fig. 21. An ε-amino caproic acid linker was utilized at the carboxy termini of each of these classes of molecules to give directionality to the molecules. The monomer through octamer chain lengths for each anomer were synthesized, and several techniques were utilized to evaluate their secondary conformational characteristics.

The synthesis and characterization of the secondary structure of the (1→5)-amide linked β-methoxy sialooligomers, was reported by our research group in 1998.[62] In that paper, we proposed a stable secondary structure for the higher order oligomers, based upon CD results, in conjunction with NMR and molecular modeling studies. These molecules were the first reported δ-amino acid 'foldamers'[18] shown to be water-soluble, and the first carbohydrate-based amide-linked compounds shown to have secondary structure in water. We performed our CD analysis with the assistance of Professor Edwin R. Morris, of

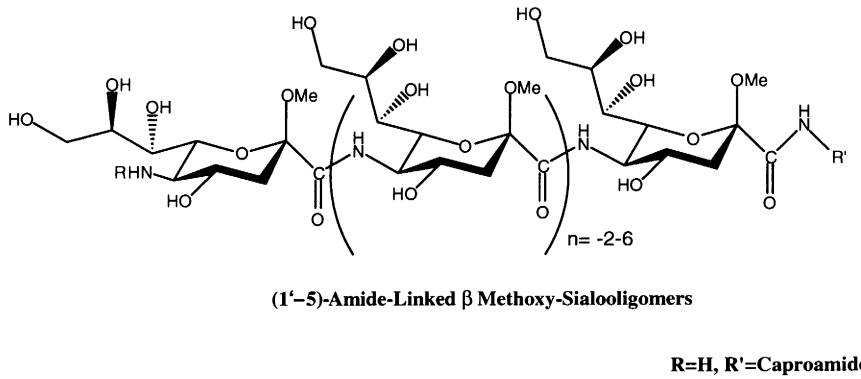


Fig. 21. Structures of the β-methoxy amide-linked sialooligomers produced in our laboratory

Cranfield University in the UK, who is an expert in polysaccharide CD. Our CD results are revealed in Fig. 22, with the legend and peak-to-trough analysis appearing in the table. The molar ellipticities for the oligomers at each wavelength have been divided by the number of residues to determine the contribution of each additional residue to the stability of the secondary structure(s).

When we evaluated the CD of these molecules, some interesting features were noted. First, the monomer unit, complete with the caproic acid linker, did not display the positive CD band at approximately 200 nm, characteristic of the other oligomer lengths. This is similar to the results presented by Bystricky and co-workers, when they recorded the CD of both colominic acid and the *N*-deacetylated polymer, and found the positive $n\rightarrow\pi^*$ transition band lacking in the deacetylated polymer. They were therefore able to assign the positive band to the *N*-acetyl chromophore.[52] In much the same way, the positive band at approximately 200 nm was attributed to the $n\rightarrow\pi^*$ transition of the interresidue amide bond. The negative band at approximately 220 nm was fairly consistent between all chain lengths, including the monomer, ranging from $-1.81$ to $-2.26$ deg cm$^2$/dmol. This transition may also be an $n\rightarrow\pi^*$ transition, arising from the amide chromophores in the caproamide linker. This would explain why all of the oligomers have approximately the same molar ellipticity values for this band.

The peak-to-trough ratios for the amide-linked sialooligomers were also evaluated. Starting with the dimer, the P–T ratio increased from the monomer to dimer, and also from the dimer to trimer. The tetramer through hexamer all had roughly the same peak-to-trough ratio, 10.9. This suggested that these three molecules displayed similar secondary structures. At the heptamer level, the ratio increased indicating a change in the conformation of the molecule. The octamer followed suit, with the ratio increasing further. These peak-to-trough results differ from those of the glycosidically linked oligosaccharides, where the ratio increased and then decreased upon oligomer elongation. The amide-linked sialooligomer P–T ratios steadily increased up to the tetramer length. There appear to be similar structural features for the tetramer through the hexamer, with conformational change being apparent in the heptamer and octomer. The formation of a stable secondary structure at the level of the tetramer is analogous to the γ-peptides reported by Hanessian and co-workers,[25] and the β-peptides of Gellman and associates.[19,20] The NH/ND exchange for the amide protons using simple one-dimensional $^1$H NMR was also evaluated to further elucidate the structures of these oligomers.

Kinetic measurements of NH/ND exchange for each oligomer in DMSO-$d_6$ in the presence of 10% $D_2O$ were performed. The results of these experiments are presented in Table 3, and are consistent with the CD data. The half-life of the internal amides is approximately the same for the tetramer through the hexamer. Interestingly, in the heptamer, the amide protons exchange relatively rapidly. The relatively fast exchange rates of the heptamer indicate that hydrogen bonding in this particular oligomer is not protected

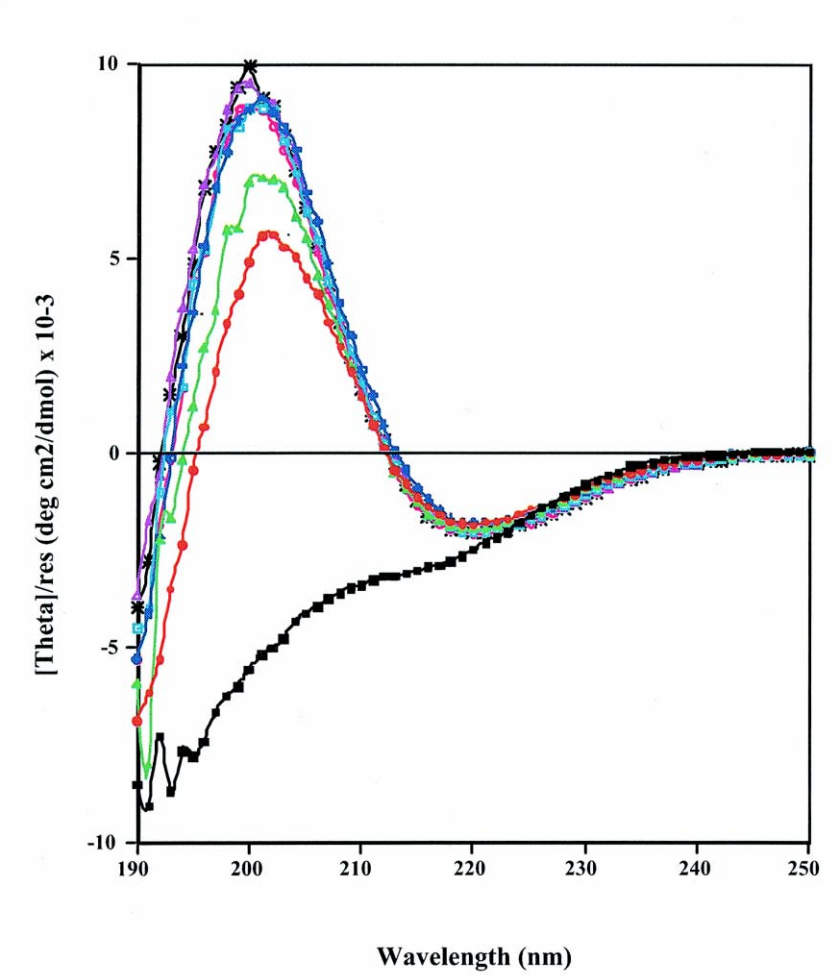


| | Chain Length | Peak Max | Peak Min | Peak - Trough |
|---|---|---|---|---|
| ■ | Monomer | -5.160 | -2.256 | -2.904 |
| ● | Dimer | 5.623 | -1.838 | 7.461 |
| ▲ | Trimer | 7.051 | -1.961 | 9.012 |
| ✣ | Tetramer | 9.102 | -1.810 | 10.912 |
| ❑ | Pentamer | 8.882 | -2.024 | 10.906 |
| ❍ | Hexamer | 8.852 | -2.081 | 10.933 |
| Δ | Heptamer | 9.489 | -1.974 | 11.463 |
| ✳ | Octamer | 9.936 | -1.994 | 11.930 |

Fig. 22. CD spectra of the (1→5)-amide linked β-methoxy sialooligomers from monomer through octamer. The table shows the corresponding peak-to-trough analysis for the sialooligomers. The units for all numerical values are (deg $cm^2$/dmol)$\times 10^{-3}$

from the solvent. This suggests that the heptamer is in conformational flux compared with the other chain lengths that appear to have stable secondary structures. The NH/ND exchange results match the CD data, indicating that a change in the secondary structure of the molecule occurs at the heptamer level. At the octamer, slow exchange of the amide protons is observed; however the CD data clearly differ from shorter oligomers. These combined data suggest that the octomer adopts a different secondary structure than the tetramer through hexamer series. A combination of these two conformations may be available to the heptamer, which would explain its conformational flux.

Table 3
The $t_{1/2}$ (h) determined by NH/ND exchange experiments. n/o=Not observed

| | | Internal Amides | | | | |
|---|---|---|---|---|---|---|
| Oligomer | Linker 2° Amide | End Amide | End - 1 | End - 2 | Linker 1° Amide | Linker 1° Amide |
| Monomer | 43.0 | n/a | n/o | n/o | 7.3 | 7.7 |
| Dimer | 20.0 | 0.5 | n/o | n/o | 1.8 | 1.9 |
| Trimer | 67.0 | 1.0 | 7.0 | n/o | 5.8 | 5.3 |
| Tetramer | 45.0 | 1.0 | 8.3 | 6.2 | 4.6 | 5.0 |
| Pentamer | 52.0 | n/o | 10.8 | | 4.8 | 4.7 |
| Hexamer | 63.0 | n/o | 11.6 | | 5.0 | 4.9 |
| Heptamer | 11.0 | n/o | 1.3 | | 2.2 | 2.6 |
| Octamer | 58.0 | n/o | 10.4 | | 4.8 | 4.9 |

Based upon the CD and NMR results, a model of the secondary structure present in the higher order β-methoxy sialooligomers has been proposed (Fig. 23). The arrows in green indicate a $3_{16}$ helical pattern, the 3 indicating the number of residues per turn, and the 16 representing the size of the ring formed. This structure is possible for the tetramer and higher order oligomers. The tetramer is the first oligomer with an internal amide capable of hydrogen bonding back to the linker 2° amide proton. This secondary structural pattern predominates from the tetramer through the hexamer. At the heptamer chain length a second type of hydrogen-bonding pattern is possible, that is indicated by the red arrows. This structure represents a $4_{22}$ helical pattern. It appears that at the heptamer length, both secondary structures are plausible, whereas for the lower order oligomers, the $3_{16}$ helix predominates. When the oligomer reaches the octamer chain length, the $4_{22}$ helix may become the more dominant pattern as evidenced by the restoration of the shielding of the amide protons from the solvent, and the increase in the P–T ratio in the CD.

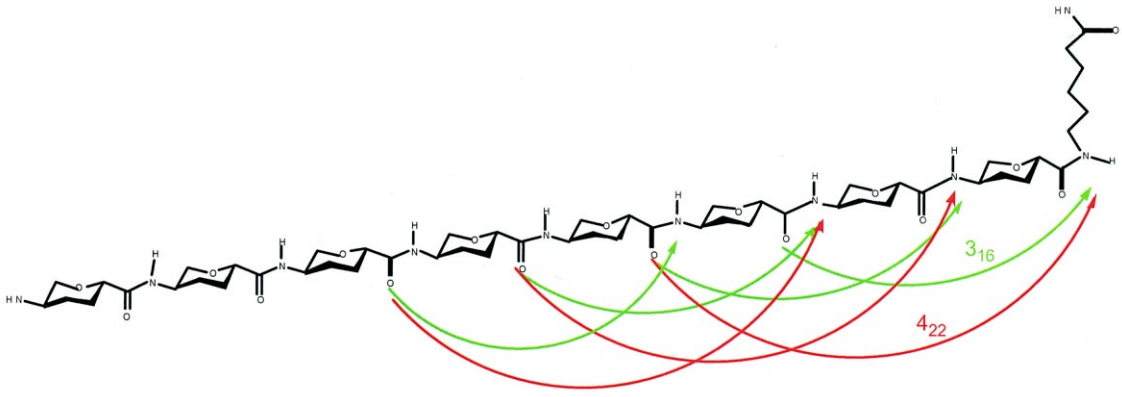


Fig. 23. Proposed hydrogen-bonding patterns that dictate two different, chain-length dependent, stable secondary structures. The shorter arrows indicate the $3_{16}$ helix, and the longer arrows illustrate the $4_{22}$ helix

The conformations of the oligomeric sialooligomers were also modeled using MacroModel™ and the Amber force field. The structure obtained by these means corroborated the model helical structure that was consistent with the $3_{16}$ helix. This structure is illustrated in Fig. 24.

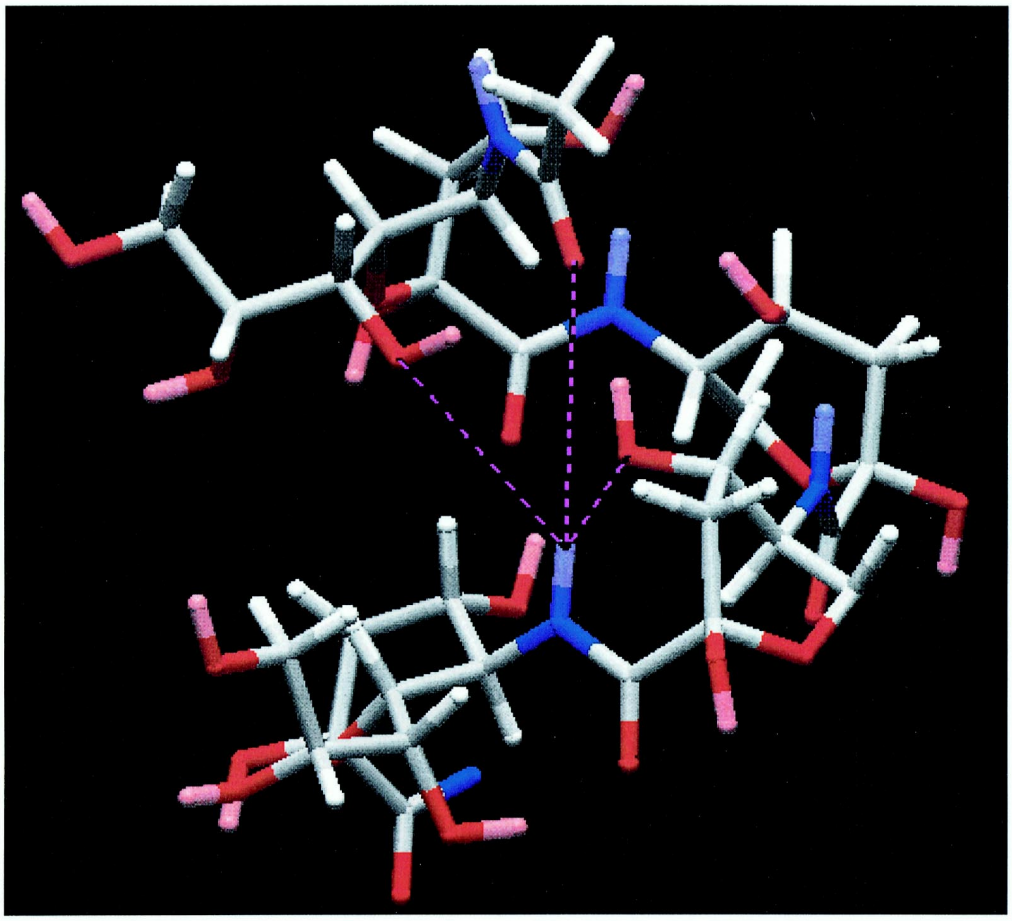

Fig. 24. MacroModel™-generated helical structure for the β-methoxy amide-linked sialooligomers

The current hypothesis for the secondary structures of the (1→5)-amide-linked β-methoxy sialooligomers is that a stable $3_{16}$ helix exists in the tetramer through the hexamer. The heptamer has the possibility of two different hydrogen-bonding patterns, which give rise to either a $3_{16}$ helix or a $4_{22}$ helix. It is this propensity of the heptamer that led to the change in molar ellipticity seen in the CD, which was correlated with a diminished half-life for all of the amide protons in the molecule. For the octamer, it appears the more extended $4_{22}$ helix becomes predominant, as evidenced by the change in the molar ellipticity in the CD, as well as the restoration of longer half-lives for the amide protons. These molecules are currently under further structural investigation in our group, in order to more clearly define their secondary structural properties.

## 5. Conclusions

In conclusion, CD is a very powerful technique that can be utilized to help probe the secondary structural characteristics of interesting oligomeric and polymeric molecules in solution. CD in conjunction with other techniques such as NMR and molecular modeling has been successfully used to gain a clearer picture of the hydrogen-bonding interactions, and conformational information of molecules that are not accessible by X-ray crystallography. The use of the peak-to-trough analysis within each class of oligomers has been an integral part of the analysis, and has provided interesting insights into the conformational changes that occur within oligomers with varied chain lengths. Continued studies in this relatively new area of research will add to the knowledge base that correlates circular dichroism data with other spectroscopic techniques ultimately facilitating secondary structure characterization. One important goal is to achieve a standardized method for the analysis of unnatural oligo- and polymeric compounds using CD in much the same manner that natural peptides and proteins can be analyzed today.

## Acknowledgements

Financial support for this research was gratefully received from NIH (AI40359-02), Eli Lilly, Alfred P. Sloan Foundation, and The National Science Foundation Early Career Award (CHE9623583). K.D.M. gratefully acknowledges receipt of the University of Arizona Dean's Fellowship and the Department of Chemistry Carl S. Marvel Fellowship. We are most grateful to Edwin R. Morris for his guidance in the CD studies.

## References

1. Yang, J. T.; Wu, C.-S. C.; Martinez, H. M. *Calculation of Protein Conformation from Circular Dichroism*; Academic Press: 1986; Vol. 130, pp. 208–269.
2. Holzwarth, G. M.; Doty, P. The Ultraviolet Circular Dichroism of Polypeptides. *J. Am. Chem. Soc.* **1965**, *87*, 218.
3. Morris, E. R. *Chiroptical Methods*; Ross-Murphy, S. B., Ed.; Blackie Academic & Professional: London, 1994; pp. 15–64.
4. Bystricky, S.; Szu, S. C.; Gotoh, M.; Kovac, P. Circular Dichroism of the *O*-Specific Polysaccharide of *Vibrio cholerae* O1 and Some Related Derivatives. *Carbohydr. Res.* **1995**, *270*, 115–122.
5. Johnson Jr., W. C. Protein Secondary Structure and Circular Dichroism: A Practical Guide. *Proteins: Struct., Funct., and Genetics* **1990**, *7*, 205–215.
6. Woody, R. W. *Circular Dichroism*; Academic Press: San Diego, 1995; Vol. 246, pp. 34–70.
7. Woody, R. W. *Theory of Circular Dichroism of Proteins*; Fasman, G. D., Ed.; Plenum Press: New York, 1996; pp. 25–67.
8. Venyaminov, S. Y.; Yang, J. T. *Determination of Protein Secondary Structure*; Fasman, G. D., Ed.; Plenum Press: New York, 1996; pp. 69–107.
9. Johnson, W. C. J. Secondary Structure of Proteins Through Circular Dichroism Spectroscopy. *Ann. Rev. Biophys. Chem.* **1988**, *17*, 145–166.
10. Johnson, W. C. J. *The Circular Dicroism of Carbohydrates*; Horton, D., Ed.; Academic Press: San Diego, 1987; Vol. 45, pp. 73–124.
11. Stevens, E. S. *Carbohydrates*; Fasman, G. D., Ed.; Plenum Press: New York, 1996; pp. 501–530.
12. Rees, D. A.; Morris, E. R.; Thom, D.; Madden, J. K. *The Polysaccharides*; Aspinall, G. O., Ed.; Academic Press: New York, 1982; Vol. 1, p. 195.
13. Wiesler, W. T.; Berova, N.; Ojika, M.; Meyers, H. V.; Chang, M.; Zhou, P.; Lo, L.-C.; Niwa, M.; Takeda, R.; Nakanishi, K. 55. A CD-Spectroscopic Alternative to Methylation Analysis of Oligosaccharides: Reference Spectra for Identification of Chromophoric Glycopyranoside Derivatives. *Helv. Chim. Acta* **1990**, *73*, 509–551.
14. Engle, A. R.; Purdie, N.; Hyatt, J. A. Induced Circular Dichroism Study of the Aqueous Solution Complexation of Cello-Oligosaccharides and Related Polysaccharides with Aromatic Dyes. *Carbohydr. Res.* **1994**, *265*, 181–195.
15. Yalpani, M. *Polysaccharides*; Elsevier: Amsterdam, 1988.

16. Chakrabarti, B. *Carboxyl and Amide Transitions in the Circular Dichroism of Glycosaminoglycans*; Brant, D. A., Ed.; American Chemical Society: Washington DC, 1981; Vol. 150, pp. 275–292.
17. Perczel, A.; Kollat, E.; Hollosi, M.; Fasman, G. D. Synthesis and Conformational Analysis of *N*-Glycopeptides. Il. CD, Molecular Dynamics, and NMR Spectroscopic Studies on Linear *N*-Glycopeptides. *Biopolymers* **1993**, *33*, 665–685.
18. Gellman, S. H. Foldamers: A Manifesto. *Acc. Chem. Res.* **1998**, *31*, 173–180.
19. Appella, D. H.; Christianson, L. A.; Karle, I. L.; Powell, D. R.; Gellman, S. H. β-Peptide Foldamers: Robust Helix Formation in a New Family of β-Amino Acid Oligomers. *J. Am. Chem. Soc.* **1996**, *118*, 13071.
20. Appella, D. H.; Christianson, L. A.; Klein, D. A.; Powell, D. R.; Huang, X.; Barchi, J. J.; Gellman, S. H. Residue-Based Control of Helix Shape in β-Peptide Oligomers. *Nature* **1997**, *387*, 381.
21. Abele, S.; Guichard, G.; Seebach, D. (*S*)-$\beta^3$-Homolysine and (*S*)-$\beta^3$-Homoserine-Containing β-Peptides: CD Spectra in Aqueous Solution. *Helv. Chim. Acta* **1998**, *81*, 2141–2156.
22. Gademann, K.; Jaun, B.; Seebach, D.; Perozzo, R.; Scapozza, L.; Folkers, G. Temperature-Dependent NMR and CD Spectra of β-Peptides: On the Thermal Stability of β-Peptide Helices — Is the Folding Process of β-Peptides Non-Cooperative? *Helv. Chim. Acta* **1999**, *82*, 1–11.
23. Daura, X.; van Gunsteren, W. F.; Rigo, D.; Jaun, B.; Seebach, D. Studying the Stability of a Helical β-Heptapeptide by Molecular Dynamics Simulations. *Chem. Eur. J.* **1997**, *3*, 1410–1417.
24. Hintermann, T.; Gademann, K.; Jaun, B.; Seebach, D. γ-Peptides Forming More Stable Secondary Structures than α-Peptides: Synthesis and Helical NMR-Solution Structure of the γ-Hexapeptide Analog of H-(Val-Ala-Leu)$_2$-OH. *Helv. Chim. Acta* **1998**, *81*, 983–1002.
25. Hanessian, S.; Luo, X.; Schaum, R.; Michnick, S. Design of Secondary Structures in Unnatural Peptides: Stable Helical γ-Tetra-, Hexa- and Octapeptides and Consequences of α-Substitution. *J. Am. Chem. Soc.* **1998**, *120*, 8569–8570.
26. Sharon, N. *Complex Carbohydrates: Their Chemistry, Biosynthesis, and Function*; Addison-Wesley Publishing: London, 1975.
27. Melton, L. D.; Morris, E. R.; Rees, D. A.; Thom, D. Conformation and Circular Dichroism of Oligosaccharides and Model Glycosides Containing Neuraminic Acid (5-Acetamide-3,5-dideoxy-D-*glycero*-D-*galacto*-nonulopyanosonic Acid) Residues. *J. Chem. Soc., Perkin Trans. 2* **1979**, 10–17.
28. Listowsky, I.; Avigad, G.; Englard, S. Conformational Equilibria and Stereochemical Relationships Among Carboxylic Acids. *J. Org. Chem.* **1970**, *35*, 1080–1085.
29. Comb, D. G.; Roseman, S. The Sialic Acids. I. The Structure and Enzymatic Synthesis of *N*-Acetylneuraminic Acid. *J. Biol. Chem.* **1960**, *235*, 2529–2537.
30. Dewitt, C. W.; Zell, E. A. Sialic Acids (*N*,7-*O*-diacetylneuraminic acid and *N*-acetylneuraminic acid) in *Escherichia coli*. II. Their Presence on the Cell Surface and Relationship to the K Antigen. *J. Bacteriol.* **1961**, *82*, 849–856.
31. Blacklow, R. S.; Warren, L. Biosynthesis of Sialic Acids by *Neisseria meningitidis*. *J. Biol. Chem.* **1962**, *237*, 3520–3526.
32. Vann, W. F.; Silver, R. P.; Abeijon, C.; Chang, K.; Aaronson, W.; Sutton, A.; Finn, C. W.; Lindner, W.; Kotsatos, M. Purification, Properties, and Genetic Location of *Escherichia coli* Cytidine-5′-Monophosphate *N*-Acetylneuraminic Acid Synthetase. *J. Biol. Chem.* **1987**, *262*, 17,556–17,562.
33. Vijay, I. K.; Troy, F. A. Properties of Membrane-Associated Sialyltransferase of *Escherichia coli*. *J. Biol. Chem.* **1975**, *250*, 164–170.
34. Troy, F. A.; McCloskey, M. A. Role of a Membranous Sialyltransferase Complex in the Synthesis of Surface Polymers Containing Sialic Acid in *Escherichia coli*: Temperature-induced Alteration in the Assembly Process. *J. Biol. Chem.* **1979**, *254*, 7377–7387.
35. Troy, F. A.; Vijay, I. K.; Tesche, N. Role of Undecaprenyl Phosphate in the Synthesis of Polymers Containing Sialic Acid in *Escherichia coli*. *J. Biol. Chem.* **1975**, *250*, 156–163.
36. Reglero, A.; Rodriguez-Aparicio, L. B.; Luengo, J. M. Polysialic Acids. *Int. J. Biochem.* **1993**, *25*, 1517–1527.
37. Rodriguez-Aparicio, L. B.; Reglero, A.; Ortiz, A. I.; Luengo, J. M. Effect of Physical and Chemical Conditions on the Production of Colominic Acid by *Escherichia coli* in a Defined Medium. *Appl. Microbiol. Biotechnol.* **1988**, *27*, 474–483.
38. Roy, R.; Pon, R. A. Efficient Synthesis of α-(2→8)-Linked *N*-Acetyl and *N*-Glycolylneuraminic Acid Disaccharides from Colominic Acid. *Glycoconj. J.* **1990**, *7*, 3–12.
39. Lindon, J. C.; Vinter, J. G.; Lifely, M. R.; Moreno, C. Conformational and Dynamic Differences Between *N. meningitidis* Serogroup B and C Polysaccharides, Using NMR Spectroscopy and Molecular Mechanics Calculations. *Carbohydr. Res.* **1984**, *133*, 59–74.
40. Griffiss, J. M. *Immunological Recognition and Effect Mechanisms in Infectious Diseases*; Torrigiani, G.; Bell, R., Ed.; Schwabe: Basel, 1981; pp. 137–152.
41. Finne, J.; Leinonen, M.; Makela, P. H. Antigenic Similarities Between Brain Components and Bacteria Causing Meningitis. *Lancet* **1983**, 355–357.

42. Sela, M.; Schechter, B.; Schechter, I.; Borek, F. *Cold Spring Harbor Symp. Quant. Biol.* **1967**, *32*, 537–545.
43. Jennings, H. J.; Roy, R.; Michon, F. Determinant Specificities of the Groups B and C Polysaccharides of *Neisseria meningitidis*. *J. Immunol.* **1985**, *134*, 2651–2657.
44. Cisar, J.; Kabat, E. A.; Dorner, M. M.; Liao, J. Binding Properties of Immunoglobulin Combining Sites Specific for Terminal or Non-Terminal Antigenic Determinants in Dextran. *J. Exp. Med.* **1975**, *142*, 435–459.
45. Michon, F.; Brisson, J.-R.; Jennings, H. J. Conformational Differences Between Linear α-(2′→8)-Linked Homosialooligosaccharides and the Epitope of the Group B Meningococcal Polysaccharide. *Biochem.* **1987**, *26*, 8399–8405.
46. Yamasaki, R.; Bacon, B. Three-Dimensional Structural Analysis of the Group B Polysaccharide of *Neisseria meningitidis* 6275 by Two-Dimensional NMR: The Polysaccharide is Suggested to Exist in Helical Conformations in Solution. *Biochem.* **1991**, *30*, 851–857.
47. Brisson, J.-R.; Baumann, H.; Imberty, A.; Perez, S.; Jennings, H. J. Helical Epitope of the Group B Meningococcal α-(2′→8)-Linked Sialic Acid Polysaccharide. *Biochem.* **1992**, *31*, 4996-5004.
48. Baumann, H.; Brisson, J.-R.; Michon, F.; Pon, R.; Jennings, H. J. Comparison of the Conformation of the Epitope of α-(2′→8)-Polysialic Acid with its Reduced and *N*-Acyl Derivatives. *Biochem.* **1993**, *32*, 4007–4013.
49. Evans, S. V.; Sigurskjold, B. W.; Jennings, H. J.; Brisson, J.-R.; To, R.; Tse, W. C.; Altman, E.; Frosch, M.; Weisgerber, C.; Kratzin, H. D.; Klebert, S.; Vaesen, M.; Bitter-Suermann, D.; Rose, D. R.; Young, N. M.; Bundle, D. R. Evidence for the Extended Helical Nature of Polysaccharide Epitopes. The 2.8 Å Resolution Structure and Thermodynamics of Ligand Binding of an Antigen Binding Fragment Specific for α-(2→8)-Polysialic Acid. *Biochem.* **1995**, *34*, 6737–6744.
50. Shimoda, Y.; Kitajima, K.; Inoue, S.; Inoue, Y. Calcium Ion Binding of Three Different Types of Oligo/Polysialic Acids as Studied by Equilibrium Dialysis and Circular Dichroic Methods. *Biochem.* **1994**, *33*, 1202–1208.
51. Jaques, L. W.; Brown, E. B.; Barrett, J. M.; Brey, W. S. J.; Weltner, W. J. Sialic Acid: A Calcium-Binding Carbohydrate. *J. Biol. Chem.* **1977**, *252*.
52. Bystricky, S.; Pavliak, V.; Szu, S. C. Characterization of Colominic Acid by Circular Dichroism and Viscosity Analysis. *Biophys. Chem.* **1997**, *63*, 147–152.
53. Yang, D.-W.; Ohta, Y.; Yamaguchi, S.; Tsukada, Y.; Haraguchi, Y.; Hoshino, H.; Amagai, H.; Kobayashi, I. Sulfated Colominic Acid: An Antiviral Agent that Inhibits the Human Immunodeficiency Virus Type I in vitro. *Antiviral Res.* **1996**, *31*, 95–104.
54. Troy, F. A.; Vijay, I. K.; McCloskey, M. A.; Rohr, T. E. *[48] Synthesis of Capsular Polymers Containing Polysialic Acid in Escherichia coli 07-K1*; Academic Press, 1982; Vol. 83, pp. 540–548.
55. Ferrero, M. A.; Luengo, J. M.; Reglero, A. HPLC of Oligo(Sialic Acids): Application to the Determination of the Minimal Chain Length Serving as Exogenous Acceptor in the Enzymatic Synthesis of Colominic Acid. *Biochem. J.* **1991**, *280*, 575–579.
56. Svennerholm, L. Quantitative Estimation of Sialic Acids. II. A Colorimetric Resorcinol–Hydrochloric Acid Method. *Biochim. Biophys. Acta* **1957**, *24*, 604–611.
57. Morris, E. R.; Rees, D. A.; Sanderson, G. R.; Thom, D. Conformation and Circular Dichroism of Uronic Acid Residues in Glycosides and Polysaccharides. *J. Chem. Soc., Perkin Trans. 2* **1975**, 1418–1425.
58. Lifely, M. R.; Gilbert, A. S.; Moreno, C. Sialic Acid Polysaccharide Antigens of *Neisseria meningitidis* and *Escherichia coli*: Esterification Between Adjacent Residues. *Carbohydr. Res.* **1981**, *94*, 193–203.
59. Gekko, K. Solvent Effects on Circular Dichroism of Colominic Acid. *Agric. Biol. Chem.* **1980**, *44*, 1183–1184.
60. Crescenzi, V.; Dentini, M.; Coviello, T. Solution and Gelling Properties of Polysaccharide Polyelectrolytes. *Biophys. Chem.* **1991**, *41*, 61–71.
61. Terabayashi, T.; Ogawa, T.; Kawanishi, Y. Negative Circular Dichroism (CD) Band of Lactones of Sialic Acid Polymers Observed at 235 nm. *Carbohydr. Polymers* **1996**, *29*, 35–39.
62. Szabo, L.; Smith, B. L.; McReynolds, K. D.; Parrill, A. L.; Morris, E. R.; Gervay, J. Solid Phase Synthesis and Secondary Structural Studies of (1′→5) Amide-Linked Sialooligomers. *J. Org. Chem.* **1998**, *63*, 1074–1078.